

Study Of Variation In The Band Gap With Concentration Of TiO_2 In $(\text{LaMnO}_3)_{1-x} / (\text{TiO}_2)_x$ (where $x = 0.0, 0.1, 0.2, 0.3$ and 0.4) Nanocomposites

Priya Thakur^{a)}, Anjna Thakur and Kamlesh Yadav^{b)}

Centre for Physical Sciences, Central University of Punjab, Bathinda-151001, India

^{a)}priyathakur1191@gmail.com

^{b)}kamlesh.yadav001@gmail.com

Abstract. In this paper $(\text{LaMnO}_3)_{1-x} / (\text{TiO}_2)_x$ (where $x = 0.0, 0.1, 0.2, 0.3$ and 0.4) nanocomposite are prepared by mixing the LaMnO_3 and TiO_2 (Sigma Chemicals, particle size ~ 21 nm) nanoparticle in appropriate ratio. These samples were characterized by using FESEM, EDS and FTIR to study the optical properties. Field Emission Scanning Electron Microscopy (FESEM) image of pure LaMnO_3 sample shows that the uniform particle size distribution is observed. The average particle size of the LaMnO_3 nanoparticles is 43 nm. The crystallite size increases from 16-24 nm with increasing the weight percentage of TiO_2 in $\text{LaMnO}_3/\text{TiO}_2$ nanocomposite up to $x=0.4$. The Fourier transform infrared spectroscopy (FTIR) spectra show that the absorption peaks appear at 450 cm^{-1} and 491 cm^{-1} which represent the Mn-O bending and Ti-O stretching mode respectively. The broadening of these peaks with increasing the concentration of TiO_2 is also observed. It gives an evidence for the formation of metal oxygen bond. The absorption band at 600 cm^{-1} corresponds to the stretching mode, which indicates the perovskite phase present in the sample. The values of band gap are found 2.1, 1.9, 1.5, 1.3 and 1.2 eV for the $x=0.0, 0.1, 0.2, 0.3$, and 0.4 respectively. Thus, the decrease in band gap and increase in refractive index with increasing concentration of TiO_2 has been observed. These prepared nanocomposites can be used in the energy applications, to make the electrical devices and as a catalyst for photocatalytic processes e.g. hydrogenation.

INTRODUCTION

Perovskite are mixed oxide having general formula (ABO_3) , where A is lanthanide element and B is manganese [1]. LaMnO_3 contains rich and fascinating physical properties because of the strong interplay lattice distortion, magnetic ordering and transport properties [2-3]. Perovskites LaMnO_3 is a ferromagnetic compound which shows ferromagnetic ordering at $T_C = 250\text{K}$. It is also used in environmental applications like the oxidation of hydrocarbon, chlorinated organic compound and H_2O_2 reactions etc. [4-6]. Titanium oxide (band gap is $\sim 3.2\text{eV}$) is the one of the most studied semiconductor for photocatalysis such as hydrogen production from water splitting and water and air treatment, due to its relatively cheap cost, non-toxicity and high chemical stability. The majority of photocatalysts are based upon wide band gap semiconductors, which are active only under UV radiation. To develop more efficient photocatalyst, there is an urgent requirement for photocatalytic systems, which are able to operate efficiently under visible light irradiation.

Perovskite-type oxides as photocatalysts have practical limitations, such as the fast electron-hole recombination that reduces the efficiency. To overcome this limitation we focus on nanocomposite of perovskites, which are advanced materials having newly gained increasing attention due to their scientific and technological importance. From a scientific point of view the composition and the atomic order of the aggregates, in addition to size, are crucial factors in determining their properties and functionalities, while the nanoscale regime convenes to them structural and degrees of freedom which are inaccessible to bulk materials. Nanocomposite materials composed of oxides and conducting polymers have brought out more fields of applications such as smart windows, toners in photocopying etc. Nanocomposites of LaMnO_3 enhances the optical properties depends upon the type of

filler. Tetsuya Kida *et al.* studied $\text{LaMnO}_3/\text{CdS}$ nanocomposite and developed a new type of visible light sensitive photocatalysts that can produce hydrogen from water containing electron donors due to reduction in the band gap [7]. Hao Huang *et al.* examined $\text{LaMnO}_3\text{-MWCNT}$ nanocomposite [8].

In this paper we report the synthesis of $\text{LaMnO}_3/\text{TiO}_2$ nanocomposite by mixing the nanoparticles of LaMnO_3 and TiO_2 in proper ratio. The prepared samples are characterized by FESEM, EDX and FT-IR. The structural and optical properties are systematically investigated.

EXPERIMENTAL WORK

LaMnO_3 nanoparticles were synthesized by sol-gel method using lanthanum nitrate, manganese nitrate and ethylene glycol as preparatory agents. The 0.2M of Lanthanum nitrate hexahydrate and 0.2M of Manganese nitrate tetrahydrate were completely dissolved in 50 ml of distilled water separately. Then mixture of 100 ml were added to the 200 ml of ethylene glycol (0.4M), stirred with a varying temperature 65-85°C for a 5 days till to form a dark homogenous mixture in continuity. The formed mixture heated in an oven at 350°C for 5 hours. During this time diffusion of metallic cations to take place and a homogeneous sol was obtained. The product was cooled to room temperature and drying at oven for 12 hours at 650°C and grinding for 2 hours. Finally the gel was calcined at 1100°C for 12 hours to obtain the pure LaMnO_3 nanoparticles. The $(\text{LaMnO}_3)_{1-x}/(\text{TiO}_2)_x$ (where $x = 0.0, 0.1, 0.2, 0.3$ and 0.4) nanocomposite are prepared by mixing the LaMnO_3 and TiO_2 (Sigma Chemicals, particle size ~ 21 nm) nanoparticle in appropriate ratio. The prepared samples were sintered at 400 °C for 2 hours. The low temperature was selected to avoid the reaction between the LaMnO_3 and TiO_2 phases. The powder was grinded for two hours and pellets were made with pellet press. Then, the as-prepared pellets were sintered at 400 °C for 2 hours. At last, the grinding of each pellet was done for 2 hours to attain the uniformity in sample [4]. The field emission scanning electron microscopy (FESEM) analysis was performed using Card Ziess Merlin Compact to investigate the morphology of prepared samples. Fourier transform infrared spectroscopy (FTIR) Bruker Tensor-27 was used in the range from 4000-400 cm^{-1} in transmission mode. The optical absorption spectra of samples as recorded at room temperature in wavelength region of 200-800 nm using UV-2450, UV spectrophotometer.

RESULTS AND DISCUSSION

FESEM Analysis

Fig.1(a-b) displays the FESEM micrographs of $(\text{LaMnO}_3)_{1-x}/(\text{TiO}_2)_x$ with $x = 0.0$, and 0.4 nanocomposite. In all samples, uniform size distribution is obtained. Fig. 1(a) shows that grains are not perfectly spherical in shape in pure LaMnO_3 sample (Calculated grain size ~ 46 nm). However, the $\text{LaMnO}_3/\text{TiO}_2$ nanocomposite image shows that the grain size is spherical in shape and highly dense morphology is observed (See Fig. 1(b)). The grain size increases from 16 to 24 nm with the increase in the concentration of TiO_2 (with $x=0.1$ to 0.4) due to the fact that nanoparticles of La MnO_3 covered with a nanoparticles of TiO_2 [9]. A decrease in grain size is observed as we go from bulk to nanocomposite. It is due to interaction between filler and matrix that yield stress tends to increase with increasing volume fraction [10]. Energy dispersive spectroscopy (EDS) analysis shows that La, Mn, Ti and O elements are present in the nanocomposite in stoichiometric ratio within the experimental error.

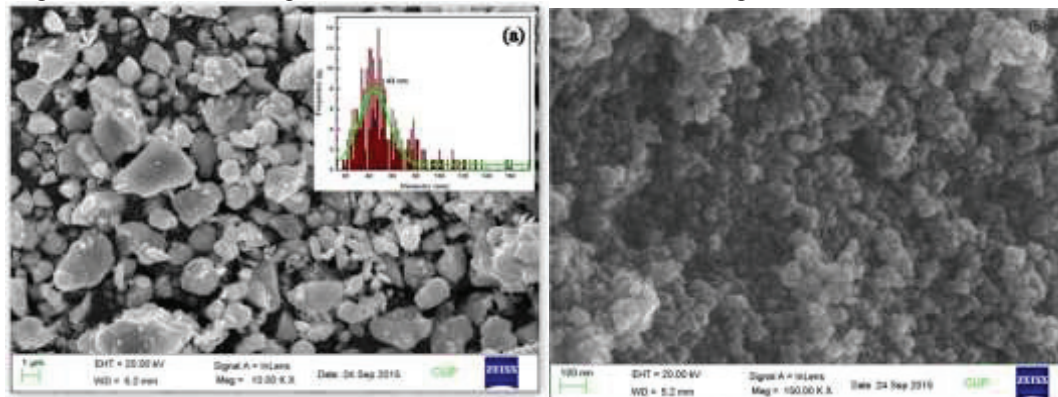


FIGURE 1. (a-b) FESEM micrograph of $(\text{LaMnO}_3)_{1-x}/(\text{TiO}_2)_x$ nanocomposite with $x = 0.0$, and 0.4.

FTIR Analysis

The FTIR spectra of LaMnO_3 and $\text{LaMnO}_3/\text{TiO}_2$ are recorded with KBr within range $400\text{--}3000\text{ cm}^{-1}$ as shown in Fig 2 (a-b). In general for pure LaMnO_3 the absorption bands appear at $750\text{--}600\text{ cm}^{-1}$, $600\text{--}450\text{ cm}^{-1}$ and $450\text{--}200\text{ cm}^{-1}$ signify the stretching, bending and wagging mode respectively. Peak appears at 446 cm^{-1} and $461\text{--}510\text{ cm}^{-1}$ in FTIR of pure sample represent the wagging and bending modes (See Fig 2(a)). The absorption band at 610 cm^{-1} corresponds to the stretching mode, which indicates the perovskite phase in the sample LaMnO_3 . It involves the internal motion of a change in the Mn-O-Mn bond length related to the MnO_6 octahedral [11].

In FTIR spectra of nanocomposite absorption peaks are present at 450 cm^{-1} and 491 cm^{-1} which represent the Mn-O bending and Ti-O stretching mode respectively (See Fig. 2(b)). The broadening of peaks with increasing the concentration of TiO_2 gives an evidence for the formation of metal oxygen bond organized in MnO_6 and TiO_6 . The intensity of absorption band increases with increase in the concentration of TiO_2 [12].

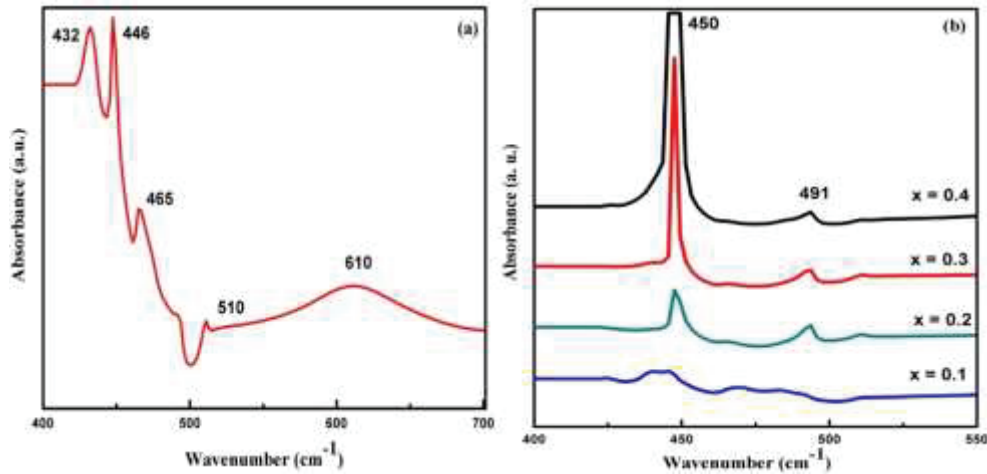


FIGURE 2. (a) FTIR spectra of pure LaMnO_3 and (b) $\text{LaMnO}_3/\text{TiO}_2$ nanocomposite with varying concentration of TiO_2 .

The optical band gap has been estimated using Tuac's equations [4]: $(\alpha h\nu)^n = A(h\nu - E_g)$, where $h\nu$ is the photon energy, α is the absorption coefficient, A is the constant relative to the material, n is both 2 for direct transition and $1/2$ for indirect transition. Hence the optical band gap for absorption peak can be achieved by the extrapolating the linear portion of the $(\alpha h\nu)^n - h\nu$ curve to zero. The direct band gap is calculated for LaMnO_3 nanoparticles is 2.10 eV as shown in Fig. 3 (a). The variation of band gap with grain size and concentration of TiO_2 is shown in Fig. 3 (b). The TiO_2 in these nanocomposites can act as an electron sink, help to separate the electron-hole pairs generated in LaMnO_3 and can reduce the recombination rate for the use in photocatalysis [13].

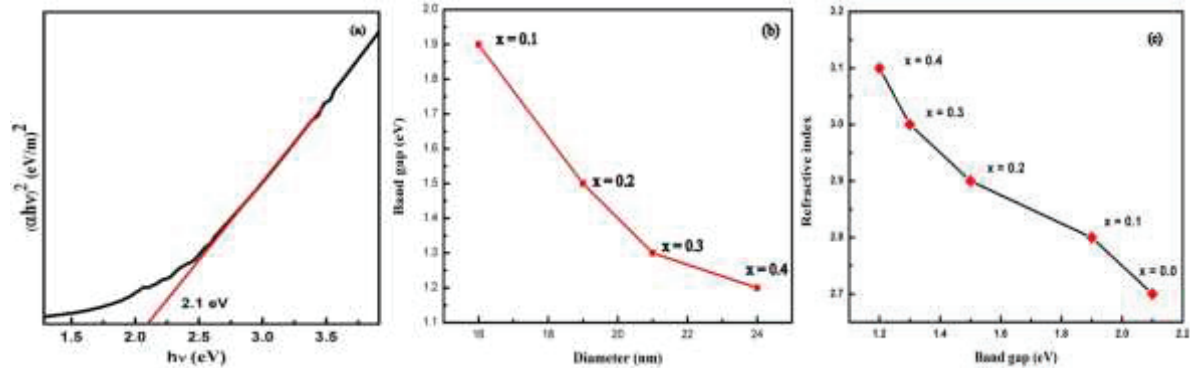


FIGURE 3. (a) The curve of $(\alpha h\nu)^n$ against $h\nu$ for the calculation of direct band gap for pure LaMnO_3 nanoparticles, (b) Variation of band gap with particle size and concentration of nanocomposite, and (c) Variation of Refractive index with band gap.

We have also calculated the refractive index of LaMnO_3 nanoparticle and $\text{LaMnO}_3/\text{TiO}_2$ nanocomposite using Moss relation [14] i.e. $n^4 = (K/\text{Band gap})$ where, K is a constant with value of 108 eV . For LaMnO_3 nanoparticles the

observed refractive index is 2.7 [15]. It is observed that the refractive index decreases with the increase in energy band gaps shown in Fig. 3 (c). The observed change in refractive index is due not only to the variation in inorganic materials but also due to the quantum size effect. In electron confinement phenomena a progressive increase in the band gap with a decrease in grain size is reported also by others [16].

CONCLUSIONS

LaMnO₃ nanoparticles have been synthesized via sol-gel method. The as-prepared nanoparticles of LaMnO₃ shows pure perovskite structure. Nanocomposite of (LaMnO₃)_(1-x)/(TiO₂)_x (x = 0.0, 0.1, 0.2, 0.3, 0.4) are successfully synthesized with average particle size 16-24 nm. The sample exhibit a broad absorption band at 450 nm. From Tauc model it has been concluded that product has a direct band gap values are found 2.1, 1.9, 1.5, 1.3 and 1.2 eV with the corresponding increase in TiO₂ (x=0.0, 0.1, 0.2, 0.3, and 0.4 respectively), which is in the range of effective photocatalysts behaviors which operate efficiently under visible light irradiation. The decrease in band gap and increase in refractive index with increasing concentration of TiO₂ have also been observed.

ACKNOWLEDGMENTS

Author (PT) is thankful to UGC, New Delhi for providing fellowship during M.Phil. One of the authors (KY) is grateful UGC, New Delhi for providing the Start-up-Grant.

REFERENCES

1. E. Hernandez^a, V. Sagredo and G.E. Delgado, *Revista Mexicana de Fisica* **61**, 166–169 (2015).
2. Sai Gong and Bang-Gui Liu, *Phys. Lett. A* **375**, 1477–1480 (2011).
3. Tokeer Ahmad, Kandalam V Ramanujachary, Samuelofland and Ashok K Ganguli, *J. Chem. Sci.* **118**, 513-518 (2006).
4. Maryam Shateriana, Morteza Enhessarib, Davarkhah Rabbanic, Morteza Asgharid and Masoud Salavati-Niasari, *Appl. Surf. Sci.* **318**, 213-217 (2014).
5. Flavia C. C. Moura, Maria H. Araujo, Jose D. Ardisson, Waldemar A. A. Macedo, Adriana S. Albuquerque, and Rochel M. Lago, *J. Braz. Chem. Soc.* **18**, 322-329 (2007).
6. Xian-Tai Zhou, Hong-Bing Ji and Xing-Jiao Huang, *Mol. Phys.* **17**, 1149-1158 (2012).
7. Tetsuya Kida, Guoqing Guan and Akira Yoshida, *Chem. Phys. Lett.* **371**, 563–567 (2003).
8. Hao Huang, Guangren Sun, Jie Hu and Tifeng Jiao, *Nanomater and Nanotech.* (P.R. China, 2014), pp. 1-5.
9. Kokkarachedu Varaprasad, Koduri Raman, G, Siva Mohan Reddy and Rotimi Sadiku, “ZnO-BiFeO₃ Nano Energy Materials for Advanced Applications,” in *IJRSET- 2014*, edited by M.R.Thansekhar et al. (ICIET’14, Tamil Nadu, India) pp. 2659-2662.
10. Nidhi Adhlakha and K.L. Yadav, *J. Mater. Sci.* **49**, 4423-4438 (2014).
11. S. Daengsakul, C. Mongkolkachit, C. Thomas, Ian Thomas and Sineenat Siri, *Rapid Commun.* **3**, 106-109 (2009).
12. Carlos Pecharroma, J. Bassas and J. Santiso and A. Figueras, *J. App. Phys.* **93**(8), 46364-4635 (2003).
13. P. Barone, F. Stranges, M. Barberio, D. Renzelli, A. Bonanno, and F. Xu, *J. Chem.* **2014**, 589707-589113 (2014).
14. L. Hannachi and N. Bouarissa, *Phys. B Condens. Matter.* **404**(20), 3650-3654 (2009).
15. S. Habouti, R. K. Shiva, C-H. Solterbeck, and M. Es-Soun, *J. App. Phys.* **102**, 044113-7 (2007).
16. Tasoula Kyprianidou-Leodidou, Walter Caseri and Ulrich W. Suter, *J. Phys. Chem.* **98**, 8992-8997 (1994).